Decreased spontaneous electrical activity in neuronal networks exposed to radiofrequency 1800 MHz signals

Corinne El Khoueiry, Daniela Moretti, Rémy Renom, Francesca Camera, Rosa Orlacchio, André Garenne, Florence Poulletier de Gannes, Emmanuelle Poque-Haro, Isabelle Lagroye, Bernard Veyret, et al.

DECREASED SPONTANEOUS ELECTRICAL ACTIVITY IN NEURONAL NETWORKS EXPOSED TO RADIOFREQUENCY 1800 MHZ SIGNALS

Corinne El Khoueiry[1], Daniela Moretti[2], Rémy Renom[1], Francesca Camera[3], Rosa Orlacchio[4], André Garenne[5], Florence Poulletier De Gannes[1], Emmanuelle Poque-Haro[1], Isabelle Lagroye[1, 6], Bernard Veyret[1, 6] and Noëlle Lewis[1]

[1] University of Bordeaux, CNRS, IMS, UMR 5218, Talence, France

[2] Center of Synaptic Neuroscience and Technology, IIT, Genoa, Italy

[3] La Sapienza University, DIET, Rome, Italy

[4]University of Rennes 1, IETR, Rennes, France

[5] University of Bordeaux, CNRS, IMN, UMR 5293, Bordeaux, France

[6] Paris “Sciences et Lettres” Research University, Paris, France

CORRESPONDENCE:

Noëlle Lewis

Email: noelle.lewis@u-bordeaux.fr

IMS Laboratory, University of Bordeaux

351 Cours de la Libération

33405 Talence cedex, France

ABSTRACT

So far, the only identified biological effects of radiofrequency fields (RF) are known to be caused by heating but the issue of potential nonthermal biological effects, especially on the central nervous system (CNS), remains open. We previously reported a decrease in the firing and bursting rates of neuronal cultures exposed to a Global System for Mobile (GSM) RF field at 1800 MHz for 3 min (Moretti et al. 2013). The aim of the present work was to assess the dose-response relationship for this effect, and also identify a potential differential response elicited by pulse-modulated GSM and continuous-wave (CW) RF fields. Spontaneous bursting activity of neuronal cultures from rat embryonic cortices was recorded using 60-electrode Multi Electrode Arrays (MEAs). At 17-28 days *in vitro*, the neuronal cultures were subjected to 15-min RF exposures, at SARs (Specific Absorption Rates) ranging from 0.01 to 9.2 W/kg. Both GSM and CW signals elicited a clear decrease in bursting rate during the RF exposure phase. This effect became more marked with increasing SAR and lasted even beyond the end of exposure for the highest SAR levels. Moreover, the amplitude of the effect was greater with the GSM signal. Altogether, our experimental findings provide evidence for dose-dependent effects of RF signals on the bursting rate of neuronal cultures and suggest that part of the mechanism is nonthermal.

Keywords: *in vitro*; neuronal cultures; radiofrequency fields; GSM-1800 signal; bursting rate.

NEW & NOTEWORTHY

In this study, we investigated the effects of some RF exposure parameters on the electrical activity of neuronal cultures. We detected a clear decrease in bursting activity, dependent on exposure duration. The amplitude of this effect increased with the SAR level and was greater with GSM than with CW signal, at the same average SAR. Our experiment provides unique evidence of a decrease in electrical activity of cortical neuronal cultures during RF exposure.

INTRODUCTION

The rapid development of wireless communications has raised questions about potential increased health risks related to exposure to radiofrequency fields (RF). The close proximity between the mobile phone and the brain of the user, combined with the fact that neurons are excitable cells, make the central nervous system (CNS) a potential target of RF exposure. Absorption of RF fields by biological tissues is quantified using the Specific Absorption Rate (SAR) metric, expressed in watts per kilogram (W/kg), which represents the absorbed power per unit of tissue mass. Two types of RF effects may occur: thermal or nonthermal. The former, which are prominent in case of high-level RF exposures, are well established and understood, while the latter are still controversial (SCENIHR 2015). In this context, several human electroencephalography (EEG) studies have reported variations in the EEG power spectrum during and/or after RF exposure, in resting EEG and during sleep (Van Rongen et al. 2009; SCENIHR 2015), suggesting that RF exposure may directly influence brain dynamics. However, the mechanisms underlying these effects on the EEG are still unknown. Therefore, it was deemed necessary to study the spontaneous electrical activity of neuronal networks *in vitro,* both at cellular and network levels, in order to detect effects of low-level RF on the nervous system.

Our research group previously published an *in vitro* pilot study on neuronal networks exposed to a Global System for Mobile (GSM) signal at 1800 MHz (Moretti et al. 2013). The GSM signal refers to the initial development of digital mobile communication systems (2G). It is a TDMA (Time Division Multiple Access) communication protocol. The pure carrier frequency emission is referred to as CW (for Continuous Wave) while the GSM signal is a pulsed-modulated signal at 217 Hz with a 1/8 duty cycle. In that previous study, a novel method was used to record neuronal extracellular electrical activity under RF exposure. A 30% reversible decrease in firing and bursting rates was found during 3-min GSM 1800 MHz exposures of neuronal cultures from rat embryonic cortices (15-21 days *in vitro*). The reported SAR of 3.2 W/kg was later recalibrated to 4.6 W/kg. To our knowledge, there has been no new report on exposure in the GHz frequency range of neuronal networks since Moretti et al. (2013).

The research presented here aimed to achieve more precise characterization of the previously published effect, in terms of dose-effect and potential differential effect between pulsed (GSM) and

non-pulsed (CW) RF signals. This involved assessing the amplitude of the effect as a function of SAR, electric field (E), and RF signal type (i.e. CW or GSM). The effects of all GSM and CW exposures were compared at the same averaged SAR, so that the total energy transferred to the sample was identical and the temperature elevation of the culture medium was the same. Data were also plotted against the averaged E. The exposure protocol consisted of 15-min RF at bulk SARs ranging from 0.01 to 9.2 W/kg, compared to sham conditions.

MATERIAL AND METHODS

Cell culture

To collect electrical activity, primary neurons were cultured on commercial microelectrode arrays (MEAs) as described previously (Moretti et al. 2013). Polyethyleneimine (PEI) or polylysine (PLL) (Sigma–Aldrich, St. Quentin-Fallavier, France) were used to coat the active area of the MEA to promote attachment of neurons in the primary cell culture. These two coating methods have been tested in order to spread over time the maturity of the neuron cultures, as cultures grown on PEI are maturing sooner than neurons cultured on PLL. Laminin (Sigma–Aldrich, St. Quentin-Fallavier, France) was also added on top of the PEI and PLL coatings for better adherence.

The primary neuronal cell cultures were obtained from the cortex of embryonic (E18) Sprague–Dawley rats (Charles River Laboratories, L'Arbresle, France). After 5% isoflurane anesthesia, the gestating rat was sacrificed by elongation. Embryos cortices were dissected in Dulbecco's Modified Eagle Medium (DMEM)-penicillin/streptomycin (Fisher Scientific, Illkirch, France), and treated for 30 min with an enzymatic solution containing 20 units/ml of papain and 0.005% of DNase (Worthington Biochemical Corporation, Lakewood, Colorado, USA). The fragments were then subjected to mechanical dissociation using a 10-ml serological pipette and centrifuged at 300 g for 5 min at room temperature. The supernatant was eliminated and the pellet was placed in suspension in a solution containing DNase. This latter mixture was placed above an albumin-inhibitor solution, to create a discontinuous density gradient, and then centrifuged at 70 g for 6 min at room temperature. In this last step, the dissociated cells (in the pellet) were separated from membrane fragments of dead cells in the supernatant. Finally, the pellet containing cortical cells was suspended in the culture medium

composed of neurobasal medium supplemented with 2% B-27, 1% GlutaMAX, and 1% penicillin/streptomycin (Fisher Scientific, Illkirch, France). Each MEA was plated with a suspension of 10^5 cells and kept until recording in a 5% CO_2 incubator at 37 °C in a humidified atmosphere. The culture medium was changed three times a week.

Acquisition system

Neuronal networks were grown in culture chambers that were constituted of a 6 mm-high glass cylinder sealed with biocompatible silicone on a 60-channel planar MEA from Qwane Biosciences (Qwane, Lausanne, Switzerland) that was used as electrophysiological interface as previously described (Moretti et al. 2013). These biochips are built on 15 x 15 mm glass substrates mounted on printed circuit boards (PCB; 50 x 50 mm) using standard microfabrication technologies. They provide 60 platinum electrodes (200 µm spaced with 40 µm diameter tips). To allow the insertion of the culture chamber inside the exposure system, the pre-amplifier (MEA1060-Inv, Multi-Channel Systems (MCS), Reutlingen, Germany) had to be placed underneath the MEA; we thus had custom MEAs built by Qwane Biosciences, in which the contact pads were placed on the bottom side of the PCB.

Exposure setup and RF signals

The exposure setup for electrophysiological recording comprised the MEA and an open Transverse ElectroMagnetic cell (TEM), consisting of a rectangular coaxial transmission section tapered towards the coaxial connectors on both sides, as shown in Fig. 1. A. The inner conductor, or septum, acted as the positive conductor or hot line. The outer conductor acted as the ground. The impedance along the TEM cell was 50 Ω, so a matched 50 Ω load was placed at the output port. The MEA glass cylindrical chamber was inserted into the TEM cell through a 14.5 mm-diameter circular hole in the ground plate. The TEM cell was connected to an RF generator-amplifier as a source of GSM and CW signals at 1800 MHz (RFPA, Artigues-près-Bordeaux, France).

RF exposure is characterized by SAR, quantifying the energy deposited in a tissue. SAR, expressed as W/kg, is the physical quantity that causes tissue heating with RF exposure. In this study, we

compared exposure to GSM and CW signals, which have different modulation profiles, as shown in Fig. 1. B. The effects of GSM and CW exposure are usually compared at the same time-averaged SAR, to ensure the same amount of heating. Due to the pulsed nature of GSM signal, with a 1/8 duty-cycle, its peak power SAR is eight times greater than that of the equivalent CW signal (Fig. 1. B).

Dosimetric modeling of the exposure system that was used in these experiments has been described previously (Merla et al. 2011; Moretti et al. 2013). The temperature elevation of the culture medium had been measured in the dosimetry study (Merla et al. 2011): it reached 0.6 °C at 15 min, during a 7.4 W/kg exposure. In our experiments, the medium temperature elevation at a given SAR level was estimated from these reference measurements. For example, for a 15-min RF exposure at 9.2 W/kg, the temperature increase was estimated at 0.7 °C.

To avoid any bias concerning the thermal or non-thermal nature of the mechanism, the dose response was plotted as a function of the time-averaged SAR, as well as the time-averaged electric field E. SAR is related to E as follows: $SAR = \sigma E^2/\rho$, where σ is the conductivity of the culture medium (2.12 S/m at 1800 MHz; Merla 2011), E the electric field in V/m and ρ the density of the medium (1000 kg/m^3). For the CW signal, as the SAR and E values are constant, the average $E = E_{CW} = \sqrt{\rho SAR/\sigma} = 21.7\sqrt{SAR}$ Due to the 1/8 duty-cycle for GSM (Fig.1. B), the relationship between the average E of GSM and CW signals with the same average SAR is: $E_{GSM} = 1/\sqrt{8}\, E_{CW}$. SAR and E always refer below to time-averaged SAR and E, respectively.

Electrophysiological recordings

In order to maintain the proper cell culture conditions during the recordings, the experiments were carried out in a dry incubator (37 °C, 5% CO_2) where the pre-amplifier, the MEA, and the exposure system were placed. The MEA culture chamber was sealed with a removable membrane made of fluorinated ethylene-propylene (ALA Scientific Instruments, New York, USA) to prevent evaporation while allowing for gas exchange. The pre-amplification gain was 1200 and a shielded cable was used to transfer data from the preamplifier, inside the incubator, to a desktop computer equipped with an

MCS-dedicated data-acquisition board. Raw data were sampled at 10 kHz/channel. Signals were recorded and monitored using the MC Rack software (MCS) for on-line visualization and raw-data storage.

Signal Processing and burst detection

The electrical activity of neuronal cultures was analyzed using the SPYCODE software (Bologna et al. 2010). Spiking activity was detected with the differential-threshold precision-timing spike-detection method (PTSD) (Maccione et al. 2009). It detects a spike when the peak-to-peak amplitude of the signal exceeds eight times the standard deviation (SD) of the biological noise in a 2 ms sliding window. The SD of the biological noise was evaluated for each recording channel in the pre-exposure phase. Then, bursts were detected using the method described by Pasquale et al. (2010). The algorithm is based on the computation of the logarithmic inter-spike interval (ISI) histogram and automatically detects the best threshold for distinguishing between inter- and intra-burst ISIs, for each recording channel of the array. An analog thresholding method was used to detect network bursts, based on inter-burst interval (IBI) histogram combined with a synchronization criterion implicating a given amount of the total electrodes (20% generally) (Pasquale et al. 2010).

In our previous study (Moretti et al. 2013), several metrics were analyzed: spike firing rate, mean bursting rate (MBR), duration of bursts, number of bursting channels, network bursts, inter-spike interval, and inter-burst interval. Since the amplitude of the effect was higher for the MBR, this metric was used to investigate the role of the various exposure parameters. MBR is the average number of bursts per minute collected over the burst-active electrodes (defined as yielding at least one burst during the recording).

At the end of the analysis, we extracted raster plots representing spikes, bursts, and network bursts for each recording, and a visual control was performed for each data file. In total, 17 recordings out of 104 were eliminated from the final results as they exhibited fewer than 10 bursts per minute at the beginning of the recording (phases S1 and S2).

As expected from the dosimetry study (Merla et al. 2011), the electromagnetic field created an interference on the electrodes, resulting in a recorded artifact during GSM exposure. This artifact, with the time profile of the GSM 217 Hz modulation, had already been observed and managed in our previous study (Moretti et al. 2013). Its maximum amplitude was on the order of 1 mV and it had to be eliminated before spike detection. As explained in (Moretti et al. 2013), we implemented a stop-band filter to remove it without altering the electrophysiological signal; a set of 30 stop-band filters, each centered on one artifact harmonic frequency (from 217 Hz to 6510 Hz) was built using Matlab and integrated in SPYCODE, in the pre-processing section. The impact of this added filter was tested positively for removing the artifact and preserving the spikes (Moretti et al. 2013). This GSM-filter was systematically applied to the recorded signals, with or without RF exposure.

Exposure protocol

The neuronal networks were exposed between 17 and 28 days *in vitro* (DIV); in this age range, the neuronal activity is balanced between random spikes and bursts (Chiappalone et al. 2005; Van Pelt et al. 2005). In all experiments, after placing the MEA in the recording setup, we waited for the stabilization of the temperature at 37 °C inside the incubator before starting the recording, in order to work under standard cell culture conditions.

The recording protocol was adapted to assess the dose-response relationship as a function of SAR, and the potential differential response elicited by pulsed (GSM) and non-pulsed continuous wave (CW). In this protocol, the exposure phase (E) duration was 15 min, preceded by two “pre-exposure” phases (non-exposed; S1 and S2) of 15 min each, and followed by two “post-exposure” phases (non-exposed; P1 and P2) of 15 min each (Fig. 1 C).

This protocol lasted 75 min and SARs during the exposure phase ranged from 0.01 to 9.2 W/kg. A series of sham-exposures was carried out separately, using the same 5-phase protocol but with RF always OFF, in order to evaluate the baseline activity along this series of phases.

Influence of temperature elevation in the culture medium on burst activity

In our 15-min exposure protocol, the maximal SAR was 9.2 W/kg, which corresponded to a temperature elevation estimated at 0.7 °C, according to the dosimetry study (Merla et al. 2011). In order to study the potential effect of bulk heating on neuronal activity, neuron cultures were exposed during 15 min in the incubator to the heat produced by an electric hotplate (MCS). The temperature elevation in the culture medium, up to 1 °C, was monitored using a Luxtron probe (LumaSense Technologies, Erstein, France). The neuronal activity was recorded during the heating phase and the following 30-min cooling phase. The heating phase started as soon as the electric hotplate was turned on. The medium temperature reached 37.80 ± 0.03 °C after 5 min and continued increasing gradually, until it stabilized at 38 °C. After 15-min heat exposure, the hotplate was turned off and the temperature decreased rapidly to 37.30 ± 0.06 °C after 5 min, then to 37 °C for the rest of the recording.

Statistical analysis and graphs

In order to pool and compare data from different samples, we considered the MBR of the S1 phase as 100%, and we calculated the MBR of the following phases as a percentage of this value. Statistical analysis was performed using R (R Core Team, 2017) and the PMCMR library (Pohlert, 2014). We used the Friedman test followed by Conover's multiple comparison test to compare exposure protocol phases for each group (SHAM, GSM, and CW). Data are presented using whisker box diagrams. A p-value < 0.05 was considered statistically significant. In the text, data are presented as mean ± SEM. The number of samples (n) used for each analysis is mentioned in the corresponding figure caption.

RESULTS

Effect of a 15-min RF exposure at 4.6 W/kg

We first analyzed the effect of 15 min-RF exposure at a SAR of 4.6 W/kg, which was the level of exposure already used in our previous 3-min GSM exposure experiment (Moretti et al. 2013). In this 15-min exposure protocol, the recordings during the RF exposed phase (E) revealed a clear decrease in the frequency of spikes and bursts, compared to the pre-exposure recordings of spontaneous

neuronal activity (S1, S2), for both GSM and CW signals. Fig. 2 shows a typical recording of the S2, E, and P1 phases, from a 4.6 W/kg GSM exposed culture; on the raster plots, there was a marked decrease in electrical activity during the second half of the E phase and it disappeared during the first minutes of the P1 phase.

Given that the total recordings lasted 75 min, sham exposures were performed on 11 cultures in order to distinguish between variations in spontaneous activity over time and the effects of RF exposure. A spontaneous decrease of ca. 5 % in MBR was observed in each of the consecutive sham phases, with a total of 19.7 ± 14.9 % at the end of the 75-min run, but no significant difference was found within this group ($p>0.05$, Friedman test) (Fig. 3. A). For the RF exposed cultures, the MBR was corrected by systematically subtracting this average drift from the spontaneous activity in each phase.

Figure 3. B-C represents the normalized MBR for 8 GSM- and 6 CW-exposed cultures, at a SAR of 4.6 W/kg. A statistically significant difference was found within the GSM-exposed group ($p<0.001$). The MBR for the exposed phase (E) decreased significantly compared to the S1 or S2 phases ($p<0.01$). Moreover, the MBR for the P1 and P2 phases were significantly lower than those of the S1 or S2 phases ($p<0.001$), indicating that burst inhibition was not totally reversible (Fig. 3. B). The result was similar for CW exposure, with a significant difference within the group ($p<0.01$). Statistical analysis revealed that the difference was between the MBR of the E, P1, and P2 phases, compared to those of the S1 or S2 phases (Fig. 3. C).

Given the results of the statistical analysis and the extent of the effect on the E and P1 phases, we decided to group the MBR of the latter two phases, in order to compare their average MBR with the average of the S1 and S2 phases. Statistical analysis revealed a highly-significant difference ($p<0.001$) between these two groups, but also between average MBR of S1 and S2 compared to that of P2 (Fig. 3. D, E).

Dose response

We then evaluated the dose-effect relationship as a function of SAR in the 0.01 to 9.2 W/kg range, with a total of 76 MEA recordings, using both RF signals (CW, n = 35 and GSM, n = 41). Table 1 lists the SAR levels used in these experiments.

Analysis of the experiments using both signals revealed that burst inhibition was minor and reversible at low SAR (ca. 0.1 W/kg), but, at 4.6 W/kg, inhibition was present during the E phase and persisted during the P1 phase and, at 9.2 W/kg, bursting activity was completely abolished throughout the E, P1, and P2 phases.

Given the results of the statistical analysis above, we decided to quantify the decrease in MBR by evaluating the R_{MBR} ratio, comparing averaged MBR for the E and P1 phases with the averaged MBR for the S1 and S2 phases,

$$R_{MBR} = 1 - \frac{(MBR_E + MBR_{P1})/2}{(MBR_{S1} + MBR_{S2})/2}$$

where MBR_{S1}, MBR_{S2}, MBR_E, and MBR_{P1} are the MBRs during the respective phases. This ratio quantifies the relative decrease in MBR observed during (E phase) and after (P1 phase) RF exposure, with respect to a reference activity defined by the average MBR in the pre-exposure phases (S1 and S2).

Figure 4 shows the evolution of R_{MBR} as a function of SAR, for both signals. The data points were fitted using a one-parameter exponential rise function $R_{MBR} = 1 - \exp(-SAR/(1.44\ SAR_{50}))$, where SAR_{50} is the SAR value for $R_{MBR} = 0.5$ (Fig. 4). We observed that R_{MBR} increased with SAR for both GSM and CW signals. The two fitted curves were similar in shape, and total inhibition was reached at SAR ca. 9.2 W/kg for both signals. However, the SAR_{50} for the GSM signal was 0.56 that of the CW signal.

The dose response was also plotted as a function of E, the time-averaged electric field (Fig. 5). In this case, 100% inhibition was reached at 23 V/m for the GSM signal, compared to 66 V/m for the CW signal. When these curves were fitted using the exponential function, $R_{MBR} = 1 - \exp(-E/(1.44\ E_{50}))$, the fit was much better than in plots versus SAR. The E_{50} for the GSM signal was 0.29 that of the CW signal.

Since the neuron cultures were different in terms of age and coating, we investigated the role of these two parameters in the observed effect. We found no specific distribution of data points according to age or coating (data not shown), suggesting that the effect depended solely on the exposure parameters.

Influence of temperature elevation in the culture medium on burst activity

Heating by 1 °C caused slight increases in MBR during and after the E phase (Fig. 6.). This indicated that a temperature elevation at least as large as that obtained at 9.2 W/kg did not cause a decrease in MBR.

DISCUSSION

The findings described above confirm our published data on the decrease in burst activity of neuronal cultures under GSM exposure (Moretti et al. 2013). This previously reported effect was a 30% reversible decrease in MBR under 3-min GSM exposure at a SAR level of 4.6 W/kg (i.e. E = 15.9 V/m). An additional experiment repeating this 3-min exposure protocol for 3 successive times on 16 MEA neuron cultures also showed that this effect was reproducible (Moretti, thesis 2014): the inhibition of the MBR was of 30%, 41%, and 34% in the first, second, and third exposure phases, respectively, and this decrease was reversible after each of the three exposure phases. In the present study, we show that the bursting activity decreased by ca. 75% under 15-min RF exposures at the same SAR level, and this effect was not immediately reversible, for both GSM and CW signals. Moreover, at exposure levels ranging from 0.1 to 9.2 W/kg, the decrease in MBR augmented with increasing SAR (Fig. 4). At 9.2 W/kg (E_{CW} = 63.5 V/m and E_{GSM} = 22.5 V/m), a bulk SAR level at which the local SAR at the electrodes is ca. 60 W/kg (i.e. 169 V/m) (Merla et al. 2011), bursting was fully inhibited throughout the exposure and post-exposure phases. The amplitude of the effect did not depend on the age of the cultures, within the selected two-week range, or the type of coating. The decrease in bursting rate during the exposure phase and has been replicated over the years by several experimenters.

Altogether, our experimental findings provide evidence that RF signals have significant effects on the bursting rate of neuronal cultures. The amplitude of these effects was greater under exposure to pulsed GSM signals: $SAR_{50\ GSM}/SAR_{50\ CW}$ was 0.56. This was even remarkable when plotted against the electric field: $E_{50\ GSM}/E_{50\ CW}$ = 0.29.

Recorded artifact

As already mentioned in Moretti et al. (2013), an artifact appeared in the recorded signal, only in the case of GSM exposure, and was properly eliminated by the GSM filter before spike detection. Nevertheless, we needed to exclude the possibility that this interference was the direct cause of the effect. RF shielding of the amplifier resulted in a 10-fold decrease in the artifact amplitude, which suggests that its cause was mainly an interference with the pre-amplification stage. Following that operation, the artifact was masked in the noise for most electrodes and did not exceed 1 mV at the maximum SAR level (9.2 W/kg). This maximum voltage of 1 mV is however well below the threshold needed to stimulate the neurons, i.e. 1 V (Wagenaar et al. 2005; Zrenner et al. 2010). In the case of CW exposure, the power absorbed on top of the electrode was simulated in Merla et al. 2011: SAR_{CW} was ca. 30 W/kg at maximum, corresponding to an electric field E_{CW} of ca. 119 V/m. If the relevant interaction distance of this extracellular electric field with the neuron is ca. 10 µm (i.e., the thickness of the neuron), this corresponds to a 1 mV RF signal at 1800 MHz. Hence, in both CW and GSM exposures, the measured or simulated electromagnetic interference with electrodes is not likely to produce an alteration of the electrophysiological activity of the neuronal network.

Influence of temperature

It is well known that RF exposure causes temperature elevation, which can lead to biological effects. The question is whether both thermal and nonthermal mechanisms coexist. We thus investigated the role of temperature elevation in the elicitation of the effect observed on the neuronal cultures. For that purpose, we assessed the influence of temperature elevation of the culture medium (ca. 1 °C) on bursting activity: under those conditions, MBR increased slightly. While causing a similar temperature

elevation at 9.2 W/kg, RF exposure had the opposite effect; this implies that the contribution of the RF nonthermal effect was large enough to revert the heating effect completely.

RF effects on *in-vitro* neuronal activity

A very similar experimental approach was recently implemented (Oster et al. 2016), using an open TEM cell and 60-electrode MEAs. These authors published their first results on cortical neuronal networks exposed to TETRA (Terrestrial Trunked Radio) pulsed RF signals (Köhler et 2018). The signal had a carrier frequency of 395 MHz, pulsed at 17.64 Hz. In a series of 15-min TETRA exposures at 1.17 and 2.21 W/kg, no difference was found in the bursting rate before and after exposure, while increases in temperature led to an increase in bursting rate, as observed in our work. The experimental setup was not configured to record electrical activity during the exposure phase, preventing the authors from observing a potential reversible effect during TETRA exposure.

One *in-vitro* investigation assessed the effects of chronic RF exposure (15 min daily for 8 days) on synaptic function in rat hippocampus cultures, using the patch-clamp technique associated with immunohistochemistry (Xu et al. 2006). This study revealed that GSM 1800 MHz RF (2.4 W/kg, i.e. 34 V/m) caused a selective decrease in the amplitude of AMPA mEPSCs, but not in their frequency or decay time, or NMDA current amplitude. Furthermore, the authors reported a decrease in the PSD95-stained puncta, suggesting a decrease in the density of excitatory synapses after RF exposure. A parallel study by the same team, focusing on the dendritic development of cultured hippocampal neurons, also found that the number of spines decreased after the same chronic GSM exposure (Ning et al, 2007), suggesting that “low-intensity” RF exposure affected the formation of excitatory synapses in these neurons.

Other *in-vitro* investigations have used isolated neurons from ganglionic neuronal networks, a preparation considerably less complex than the cultured networks used in our experiments and the studies cited above.

Early evidence was published of the effects of RF exposure on the electrical activity of individual neurons from *Aplysia* ganglia placed within a microwave stripline (Wachtel et al., 1975). Intracellular

glass microelectrodes were used to record electrical activity during RF exposure at 1.5 GHz and ca. 1 W/kg, either pulsed (10 µs pulses at 1-5 kHz repetition rate) or CW. The largest effect was found with pacemaker neurons, which were of two types: “beating” pacemakers, with regular inter-spike intervals (ISI), and “bursting” pacemakers, with an endogenous bursting activity and regular inter-burst intervals (IBI). RF exposure increased the ISI of “beating” pacemakers, but decreased the IBI of “bursting” pacemakers. No significant difference was found between pulsed and CW exposure. Furthermore, qualitative heating tests caused the opposite effects.

In a study with a similar design, BP-4 identified neurons isolated from large parietal ganglia of *Lymnea stagnalis* were exposed in a waveguide at 900 MHz and their spontaneous electrical activity and ionic currents were recorded (Bolshakov et al., 1992). These pacemaker neurons have a small number of synaptic inputs and most of them exhibited a steady firing rate under physiological conditions. However, about 25 percent of the neurons exhibited burst-like transient irregularities. A conventional microelectrode technique was used to make intracellular recordings. The RF exposure was pulse-modulated (0.5 to 4 W/kg) or CW (0.5 to 15 W/kg). Exposure to CW RF did not influence the spontaneous electrical activity of either type of neurons. Pulsed-RF exposures within the same range of SAR caused specific changes in firing rate, independently of modulation frequency (0.5 to 110 Hz), eliciting a burst within the first minute of a 10 min-exposure in neurons that otherwise exhibited regular spiking activity. For the second type of neurons, which exhibited spontaneous burst events, the IBI decreased during exposure. The authors also studied the effect of RF exposure on ionic currents induced by activating cell-membrane ACh, DA, 5-HT, and GABA receptors and found no consistent effects. In a previous study (Bolshakov et al., 1986), the authors reported that the firing rates of *Lymnea* BP-4 neurons decreased during rapid heating and stopped completely at a rate of 0.2 °C/s.

These *in-vitro* studies on pacemaker neurons from ganglionic networks revealed an alteration in the firing patterns of neurons with endogenous firing rhythms and demonstrated that equivalent direct heating had the opposite effect on firing activity to RF exposure.

To investigate the potential mechanisms of RF-induced biological effects, we examined other reports documenting the effects of millimeter waves (MMW) on neuronal cells. MMW are usually dedicated to radar or satellite communications and use carrier frequencies in the 30–300 GHz range, i.e. much

higher than those of RF mobile phone communications. MMW cannot penetrate deeply into the body, as they are almost totally absorbed in the superficial layers of the skin within 1 mm of the surface, so they do not interact with the CNS. Consequently, the studies reported below focused on the potential effects of MMW on sensory receptors or exploitation of MMW to regulate neuronal activity.

Major but reversible electrophysiological effects were reported in patch-clamp experiments where pyramidal neurons of rat cortical slices were exposed to MMW (Pikov et al, 2010). At power densities approaching 1 μW/cm^2, 1-min MMW exposure was accompanied by MMW-induced heating of the bath solution at 3 °C and produced a considerable decrease in firing during exposure in 4 out of 8 neurons, as well as narrowing the action potential (AP) and decreasing membrane resistance. However, these effects were considerably more marked than those induced by 10°C general bath heating (Lee et al, 2005), indicating that MMW-induced effects could not be entirely attributed to heating. Moreover, blocking the intracellular Ca^{2+}-mediated signaling did not significantly alter the MMW-induced neuronal response, suggesting that MMW interact directly with the neuronal plasma membrane. This hypothesis was further examined in a second study performed by the same group, where the physiological effects of low-intensity 60 GHz RF on individual neurons in the Leech ganglia were investigated using a standard sharp-electrode electrophysiology setup (Romanenko et al, 2014). The neurons exhibited spontaneous, network-based firing activity, maintained by multiple reciprocal inhibitory and excitatory loops. During a 1-min RF exposure (incident power densities: 1, 2, and 4 mW/cm^2) or gradual bulk heating at a rate of 0.04 °C/s, the neurons exhibited a similar dose-dependent hyperpolarization of the plasma membrane and decrease in AP amplitude. However, a major difference between the effects of MMW exposure and bath heating was that the firing rate was suppressed at all MMW power densities, but increased in a dose-dependent manner during gradual bath heating. Moreover, narrowing of the AP half-width during MMW irradiation at 4 mW/cm^2 was 5 times more pronounced than during equivalent bath heating. The mechanism underlying these effects was hypothesized to involve specific coupling of MMW energy with the neuronal plasma membrane. These two *in-vitro* studies revealed that, at relatively low power exposure levels, MMW exposure modulated electrophysiological activity by decreasing or suppressing AP firing rate, in a manner similar to that found in our investigation. In another study, the same group showed that pulsed 60 GHz-MMW, with a modulation frequency between 3 and 20 Hz and a power of 64 to 550 mW, altered the spontaneous electrical activity of Leech ganglia (Romanenko et al. 2016), while the

resulting temperature elevation was, in this case, negligible (under 0.1 °C). The effects on AP were somewhat similar to those reported in their previous study, using continuous MMW (Romanenko et el. 2014): a decrease in amplitude, half-width, depolarization, and repolarization phases, reinforcing their hypothesis that MMW interacted with the plasma membrane. This conclusion was also reached over the years by the Ramundo-Orlando group who suggested that MMW affected membrane proteins and phospholipid organization in the bilayer, where water molecules seem to play an important role (Ramundo-Orlando, 2010).

In-vitro studies investigating the effects of RF exposure on neural cells and network firing activity suggested interaction mechanisms with either the plasma membrane or synapses. However, some authors published critical review of nonthermal models of interaction mechanisms, examining the effects produced directly by the applied fields (Foster, 2000 ; Apollonio 2013); they concluded that there were no plausible mechanisms for nonthermal effects. Experimentaly, the existence of nonthermal effect can be investigated by comparing the RF effects to the effects of equivalent direct heating or by comparing pulsed and non-pulsed RF exposures, at the same time-averaged SAR (Pickard et al. 1981). In the studies cited above, the results of multiple comparisons suggested that some of the RF-induced effects were not entirely thermal.

RF GSM/CW differential effects on EEG

In terms of potential RF effects on the CNS, numerous studies have revealed differential effects between pulsed and continuous RF on the electroencephalogram (EEG). An extensive review has concluded that such differential effects mainly affect the CNS (Juutilainen et al. 2011). Indeed, a number of experimental studies (human or *in vivo*) seem to have given evidence for effects of pulsed RF versus non-pulsed RF on the EEG, as developped hereafter.

RF experiments on the human nervous system have focused on cognitive function, sleep, and EEG. A thorough review of the literature yielded many reports of effects caused by exposure to RF signals of various types. EEG experiments have adopted three approaches: 1) resting EEG, 2) EEG during the various sleep phases, and 3) evoked potentials, corresponding to changes in electrical potential generated by the nervous system in response to external stimulation, or sensory or cognitive activity,

observable on the EEG recording. Many articles have been published on the effects of mobile telephony-related RF on human sleep and EEG (Kwon and Hämäläinen, 2011; reviewed in Regel et al. 2007; SCENIHR 2015). From the published literature, it may be concluded that: 1) no effect on cognitive function and hearing has been established, 2) effects on sleep have been reported but are not fully consistent among research groups, and 3) some studies have shown effects of pulsed, but not non-pulsed (CW) signals on the spectrum of EEG.

In a study of the effect of RF on spindles during sleep (Schmid et al. 2012), 30 volunteers were exposed to a 900 MHz signal, pulsed at 14 or 217 Hz for 30 min before they went to sleep. Exposure to 14 Hz significantly increased the contribution of spindles during non-REM sleep, while only a slight trend was observed at 217 Hz. These results were confirmed in a study in which 20 volunteers were exposed to a 900 MHz GSM signal at 0.6 W/kg (Loughran et al. 2012). The EEG spectral power was increased in the spindle range during non-REM sleep. In another sleep study conducted on 16 volunteers exposed to a pulsed RF signal at 0.8 Hz (Lustenberger et al. 2013), observation of the effects of RF on slow-wave activity revealed an increase following exposure to the pulsed RF signal, but not to CW. Spindle activity was not affected. Furthermore, the EEG of 72 wakeful volunteers exposed sequentially to a GSM (average SAR 0.06 W/kg) or CW (average SAR 1.95 W/kg) signal was assessed; GSM exposure caused a weakening of the alpha band, while CW was as effective as the pulsed signals (Perentos et al. 2013).

In other reports, the comparison was not possible between pulsed and non-pulsed signals. For example, 26-min 0.49 W/kg GSM exposures caused statistically significant decreases in the alpha band spectral power under closed-eyes conditions (Ghosn et al. 2015). There was no effect of 30-min, ca. 1.75 W/kg UMTS exposure, in a study on the EEG spectral power in any of the delta, theta, alpha, and beta frequency bands (Trunk et al. 2013). In a recent report, the newly deployed LTE signal (4G) was used to expose human volunteers and assess the effects on EEG. Exposure at 2.61 GHz and 1.34 W/kg (over 10 g of tissue) reduced the spectral power and the interhemispheric coherence in the alpha and beta bands of the frontal and temporal brain regions (Yang et al. 2016). Hinrikus et al. (2016) confirmed its previous work giving evidence of effects on the EEG spectrum in volunteers exposed to 450 MHz RF amplitude modulated at 7, 40, and 1000 Hz (peak SAR of 0.3 W/kg over 1 g). The authors made some hypotheses about the mechanism based on an

increased fluidity of water under RF exposure coupled with parametric excitation of some brain bioelectric processes. Independent replication and further experimental evidence will be needed to test this hypothesis.

There have been a few reports of effects of RF exposure on the nervous system of rats. Thuróczy et al. (1994) published data on the effects of whole-body RF exposure on the EEG of anesthetized rats. In that study, the total EEG spectrum increased after 10-min CW exposures at 2.45 GHz, 25 W/kg BASAR (brain-averaged SAR), but not at 8.3 W/kg. The EEG power in the delta band was augmented by localized CW exposure of the head at 4 GHz and 42 W/kg (corresponding to a temperature rise of 2 °C). The beta band was increased by exposure at 4 GHz, modulated at 16 Hz and 8.4 W/kg (non-thermal according to the authors), while the equivalent CW signal did not alter the EEG. One major limitation of this study was that the animals were anesthetized. These results suggested that a pulsed RF signal had a greater impact on EEG than CW. In López-Martín et al. (2009), rats were exposed to a GSM signal and picrotoxin, a GABA ion-channel inhibitor responsible for epileptic seizures. Exposure to RF at 0.03-0.26 W/kg resulted in a synergistic effect of picrotoxin with GSM that had a greater impact than CW.

This brief review of the literature indicates that RF exposure has indeed been shown to affect the CNS in humans (mainly EEG) and that results of animal and cell investigations support this conclusion. This suggests that neuronal networks are targets of RF, although no interaction mechanism has yet been identified. In that context*, in-vitro* experiments such as those described in this work, may contribute to identifying the molecular processes involved.

CONCLUSION

In line with our previous study, we observed *in vitro* an effect of RF exposure on the electrical activity of rat cortical neuronal networks. We focused on the dependence of this effect on average SAR or E and the pulsed nature of the RF signal. Both CW and GSM exposures elicited a clear decrease in burst rate, dose-dependent on SAR or E, but the amplitude of this effect was greater with GSM. We carefully minimized electrical interference at the electrodes and made sure that the inhibition observed was not caused by the residual artifact. Mechanisms related to the heating of the culture

medium were discounted, in coherence with others results in the literature. However, to date, we have been unable to elucidate the mechanism behind the observed RF effect on bursting activity in neuronal networks, but we may conclude that the mechanism is partly nonthermal, and is likely to involve a direct action of the electric field. In view of the differential effect detected between GSM and CW, further experiments will test combinations of exposure parameters (amplitude, repetition rate, and pulse width) to reveal their respective roles in the elicitation of the effect.

Further investigation is required to identify specific RF targets at the synaptic or plasma membrane levels. A comprehensive exploration of the RF action mechanisms on neuronal activity will be conducted on a pharmacological level. In addition, computational modeling of neuronal networks will be developed to test the various mechanistic hypotheses.

GRANTS

This work was funded by the French ANSES agency (2015- EST-15RF-19 MOTUS project).

DISCLOSURES

No conflicts of interest, financial, or otherwise are declared by the authors.

AUTHOR CONTRIBUTIONS

N.L., B.V. and I.L. conception and design of research; F.P.G., E.P-H., C.E.K., D.M. and R.R. prepared cell cultures; C.E.K., D.M., R.R. R.O. and F.C. performed experiments; C.E.K. analyzed data; C.E.K., B.V., N.L. and A.G. interpreted results of experiments; C.E.K. and B.V. prepared figures; C.E.K. and A.G. prepared statistics; C.E.K., B.V. and N.L. drafted manuscript; N.L., B.V., C.E.K. and I.L. edited and revised manuscript; all authors approved final version of manuscript.

REFERENCES

Apollonio, F., Liberti, M., Paffi, A., Merla, C., Marracino, P., Denzi, A., Marino, C., D'Inzeo, G. "Feasibility for microwaves energy to affect biological systems via nonthermal mechanisms: A systematic approach, (2013) IEEE Transactions on Microwave Theory and Techniques, 61 (5), art. no. 6478850, pp. 2031-2045

Bologna LL, Pasquale V, Garofalo M, Gandolfo M, Baljon PL, Maccione A, Martinoia S, Chiappalone M. Investigating neuronal activity by SPYCODE multi-channel data analyzer. Neuronal Netw 23:685–697, 2010.

Bolshakov MA & Alekseev SI. Bursting responses of Lymnea neurons to microwave radiation. Bioelectromagnetics 13:119-129, 1992.

Bolshakov MA, Alekseev SI**.** Electrical activity dependence of the snail pacemakers on heating rate, Biophysics 31521-523, 1986.

Kwon MS and Hämäläinen H. Effects of mobile phone electromagnetic fields: critical evaluation of behavioral and neurophysiological studies. Bioelectromagnetics 32: 253-272, 2011.

López-Martín E, Bregains J, Relova-Quinteiro JL, Cadarso-Suárez C, Jorge-Barreiro FJ, Ares-Pena FJ. The action of pulse-modulated GSM radiation increases regional changes in brain activity and c-Fos expression in cortical and subcortical areas in a rat model of picrotoxin-induced seizure proneness. J Neurosci Res 87: 1484-1499, 2009.

Loughran SP, McKenzie RJ, Jackson ML, Howard ME, Croft RJ. Individual differences in the effects of mobile phone exposure on human sleep: rethinking the problem. Bioelectromagnetics 33: 86-93, 2012.

Lustenberger C, Murbach M, Dürr R, Schmid MR, Kuster N, Achermann P, Huber R. Stimulation of the brain with radiofrequency electromagnetic field pulses affects sleep-dependent performance improvement. Brain Stimul 6 : 805–811, 2013.

Maccione A, Gandolfo M, Massobrio P, Novellino A, Martinoia S, Chiappalone M. A novel algorithm for precise identification of spikes in extracellularly recorded neuronal signals. J Neurosci Methods 177:241–249, 2009.

Merla C, Ticaud N, Arnaud-Cormos D, Veyret B, Lévêque P. Real-time RF exposure setup based on a multiple electrode array (MEA) for electrophysiological recording of neuronal networks. IEEE MTT. 59: 755-762, 2011.

Moretti D, Garenne A, Haro E, Poulletier de Gannes F, Lagroye I, Lévêque P, Veyret B, Lewis N. In vitro exposure of neuronal networks to the GSM-1800 signal. Bioelectromagnetics 34: 571–578, 2013.

Moretti D. Exposure of neuronal networks to GSM mobile phone signals. PhD Thesis, Université Sciences et Technologies, Bordeaux, France 2013 (in English) . https://tel.archives-ouvertes.fr/file/index/docid/949371/filename/MORETTI_DANIELA_2013.pdf

Oster S, Daus AW, Erbes C, Goldhammer M, Bochtler U, Thielemann C. Long-term electromagnetic exposure of developing neuronal networks: a flexible experimental setup. Bioelectromagnetics 37: 264-278, 2016.

Pasquale V, Martinoia S, Chiappalone M. A self-adapting approach for the detection of bursts and network bursts in neuronal cultures. J Comput Neurosci 29:213–229, 2010.

Perentos N, Croft R, McKenzie RJ, Cosic I. The alpha band of the resting EEG under pulsed and continuous RF exposures, IEEE BEM 60: 1702-1710, 2013.

Pickard WF and Barsoum YH. Radio-Frequency Bioeffects at the Membrane Level: Separation of Thermal and Athermal Contributions in the Characeae. Membrane Biol 61: 39-54, 1981

Pikov V, Arakaki X, Harrington M, Fraser SE, Siegel PH. Modulation of neuronal activity and plasma membrane properties with low-power millimeter waves in organotypic cortical slices. J. Neural Eng. 7: 1-9, 2010.

Pohlert T. The Pairwise Multiple Comparison of Mean Ranks Package (PMCMR), R package, http://CRAN.R-project.org/package=PMCMR}, 2014.

585 Ramundo-Orlando A. Effects of Millimeter Waves Radiation on Cell Membrane - A Brief Review. J
586 Infrared Milli Terahertz Waves 31:1400–1411, 2010.

587 R Core Team, R: A Language and Environment for Statistical Computing, R Foundation for Statistical
588 Computing, Vienna, Austria, {https://www.R-project.org/}, 2017.

589 Regel SJ, Gottselig JM, Schuderer J, Tinguely G, Rétey JV, Kuster N, Landolt H-P, Achermann P.
590 Pulsed radio frequency radiation affects cognitive performance and the waking electro-
591 encephalogram. Neuroreport 18: 803-807, 2007.

592 Romanenko S., Siegel P.H.; Wagenaar D.A., Pikov V. Effects of millimeter wave irradiation and
593 equivalent thermal heating on the activity of individual neurons in the leech ganglion. J. Neurophysiol,
594 112, 2423–2431, 2014.

595 Romanenko S, Siegel PH, Pikov V, Wallace V. Alterations in neuronal action potential shape and
596 spiking rate caused by pulsed 60 GHz millimeter wave radiation. IEEE 41st International Conference
597 on Infrared, Millimeter, and Terahertz waves (IRMMW-THz), 2016.

598 SCENIHR. Health effects of EMF – Scientific Committee on Emerging and Newly Identified Health
599 Risks, 2015.

600 Schmid MR, Loughran SP, Regel SJ, Murbach M, Bratic Grunauer A, Rusterholz T, Bersagliere A,
601 Kuster N, Achermann P. Sleep EEG alterations: effects of different pulse-modulated radio frequency
602 electromagnetic fields. J Sleep Res 21: 50-58, 2012.

603 Thuroczy G, Kubinyi G, Bodo M, Bakos J, Szabo LD. Simultaneous response of brain electrical
604 activity (EEG) and cerebral circulation (REG) to microwave exposure in rats. Rev Environ Health 10:
605 135-148, 1994.

606 Trunk A, Stefanics G, Zentai N, Kovács-Bálint Z, Thuróczy G, Hernádi I. No effects of a single 3G
607 UMTS mobile phone exposure on spontaneous EEG activity, ERP correlates, and automatic deviance
608 detection. Bioelectromagnetics 34: 31-42, 2013.

609 Van Pelt J, Vajda I, Wolters PS, Corner MA, Ramakers GJ. Dynamics and plasticity in developing
610 neuronal networks in vitro. Prog Brain Res 147:173–188, 2005.

611 Van Rongen E, Croft R, Juutilainen J, Lagroye I, Miyakoshi J, Saunders R, de Seze R, Tenforde T,
612 Verschaeve L, Veyret B, Xu Z. Effects of radiofrequency electromagnetic fields on the human nervous
613 system. J Toxicol Environ Health B Crit Rev 12:572–597, 2009.

614 Wachtel H, Seaman R, Joines W. Effects of low-intensity microwaves on isolated neurons. Ann NY
615 Academy Sci 247: 46-62, 1975.

616 Wagenaar DA, Madhavan R, Pine J, Potter SM. Controlling bursting in cortical cultures with closed-
617 loop multi-electrode stimulation. J Neurosci 25: 680-688, 2005.

618 Xu S, Ning W, Xu Z, Zhou S, Chiang H, Luo J. Chronic exposure to GSM 1800-MHz microwaves
619 reduces excitatory synaptic activity in cultured hippocampal neurons. Neurosci Lett 398: 253-257,
620 2006.

621 Yang L, Chen Q, Lv B, Wu T. Long-Term Evolution Electromagnetic Fields Exposure Modulates the
622 Resting State EEG on Alpha and Beta Bands. Clinical EEG and Neuroscience, 2016.

623 Zrenner C, Eytan D, Wallach A, Thier P, Marom S. A Generic Framework for Real-Time Multi-
624 Channel Neuronal Signal Analysis, Telemetry Control, and Sub-Millisecond Latency Feedback
625 Generation, Frontiers in Neuroscience, 4:173, 2010.

FIGURE CAPTIONS

Figure 1. A: Photograph (top), side view (middle), and top view (below) of an open transverse electromagnetic cell, showing a circular hole in the TEM cell ground plate to accommodate the MEA system. Dimensions in mm: a = 51; b = 100; c = 8; d = 12; h = 1; f = 30; g = 85; l = 14; m1 = 14.5 and m2 = 10. **B:** Top: Normalized instantaneous SAR of CW and GSM signals with the same time-averaged SAR. Bottom: Normalized instantaneous E of CW and GSM signals with the same time-averaged SAR. **C:** Time profile of the exposure protocol: S1 and S2 are control phases before exposure; P1 and P2 are control phases after exposure. The E phase corresponds to RF exposure, either GSM or CW. In the sham protocol, E corresponds to a sham exposure (no RF).

Figure 2. A: Spontaneous electrical activity of a neuron culture recorded over a 15 min-phase on a single electrode, before, during and after exposure to a GSM signal at a SAR of 4.6 W/kg. **B:** Corresponding raster plots for each phase showing the analyzed neuronal activity on a group of 22 electrodes (each one represented in a horizontal line), over the 15 min of recording (i.e. each vertical bar representing a spike, each dot representing a burst and each red bar on the bottom of the plot representing a network burst implicating the firing of more than 20% of the total electrodes). The framed line corresponds to the electrode showed on left.

Figure 3. Box plots with whiskers of normalized Mean Bursting Rate (MBR) for the RF exposed cultures, along the five phases (S1, S2, E, P1, P2) of exposure protocol. **A.** Sham exposed cultures (n=11). **B.** GSM exposed cultures (n=8) and **C.** CW exposed cultures (n=6) at SAR = 4.6 W/kg. **D. and E.** Same GSM and CW exposed cultures, shown in B and C respectively, with the MBR being averaged for S1, S2 and E,P1 phases, * $p < 0.05$, ** $p < 0.01$, $p < 0.001$***, Conover Multiple Comparison test.

651 **Figure 4.** Variation in the relative decrease in R_{MBR} as a function of SAR. Filled and open dots
652 correspond to experiments using GSM and CW signals, respectively. **A:** All data points. Nonlinear
653 regression coefficients were 0.67 and 0.77, and SAR_{50} were 1.0 and 1.8 W/kg for GSM and CW,
654 respectively. **B:** Mean points. Nonlinear regression coefficients were 0.85 and 0.89, and SAR_{50} were
655 1.3 and 1.9 V/m for GSM and CW, respectively.

656

657 **Figure 5.** Variation in the relative decrease in R_{MBR} as a function of the electric field in V/m. Filled and
658 open dots correspond to the experiments using GSM and CW signals, respectively. **A:** All data points,
659 nonlinear regression coefficients were 0.81, and E_{50} were 6.5 and 22.5 V/m for GSM and CW,
660 respectively. **B:** Mean points, nonlinear regression coefficients were 0.99 and 0.94, and E_{50} was 6.5
661 and 21.3 V/m for GSM and CW, respectively.

662

663 **Figure 6.** Standardized MBR evolution, before, during, and after heating by 1 °C. Filled data points
664 and curve represent the mean value of MBR (left Y axis), for each phase (n= 4) as indicated above
665 the graph. Grey points and curve represent the temperature elevation (right Y axis) during the
666 corresponding phases.

667

668 **TABLES**

SAR (W/kg)	**0 (Sham)**	**0.01**	**0.05**	**0.1**	**0.3**	**0.5**	**0.58**	**0.92**	**2.4**	**4.6**	**8**	**9.2**
GSM	11	2	1	6	7	0	2	1	6	8	2	6
CW		0	0	6	6	1	2	1	7	6	0	6

669

670 **Table 1.** List of the SAR levels used and the number of neuronal cultures examined at each SAR, for
671 GSM and CW signals. The gray columns correspond to the points where at least 6 recordings were
672 obtained.

A

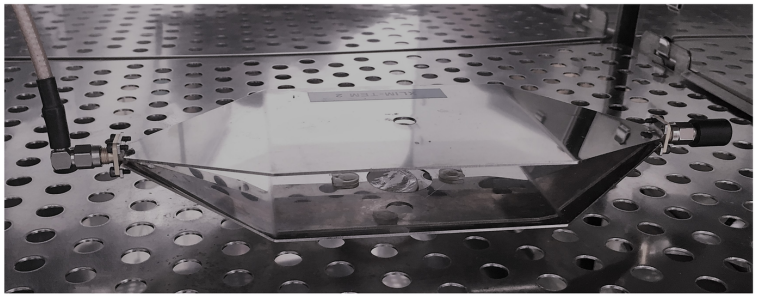

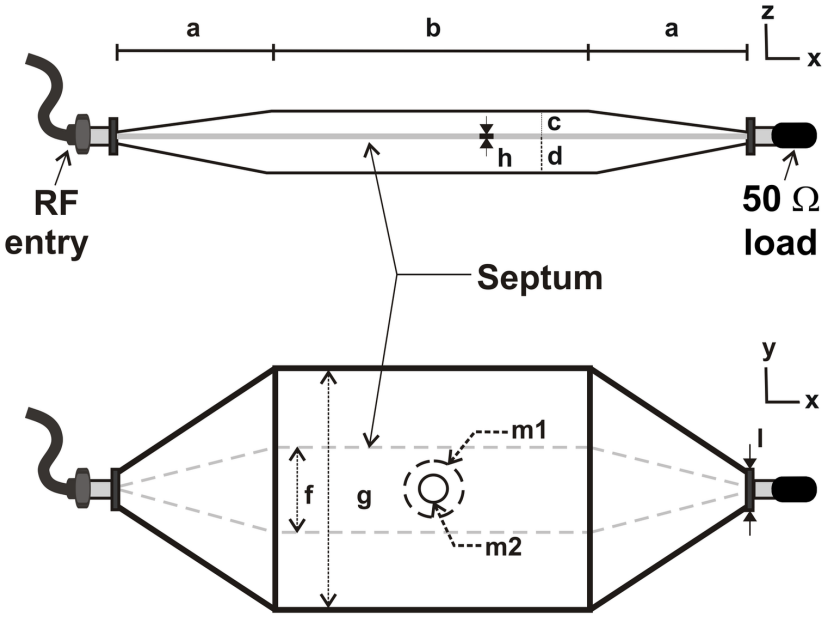
a
b
a
z
x
c
h
d
RF
entry
50 Ω
load
Septum
y
x
m1
m2
f
g
l

B

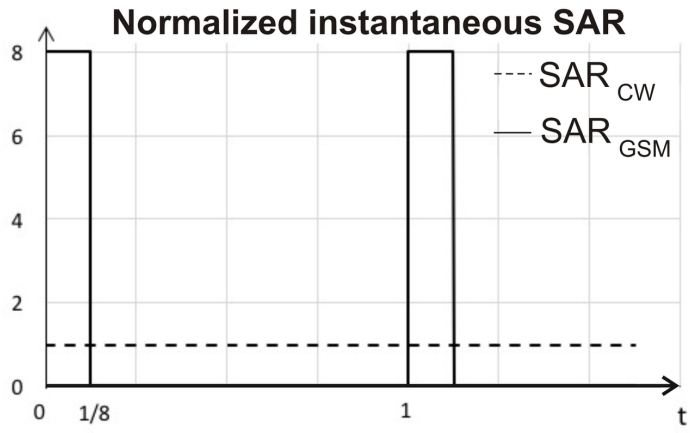
Normalized instantaneous SAR
8
6
4
2
0
SAR CW
SAR GSM
0
1/8
1
t

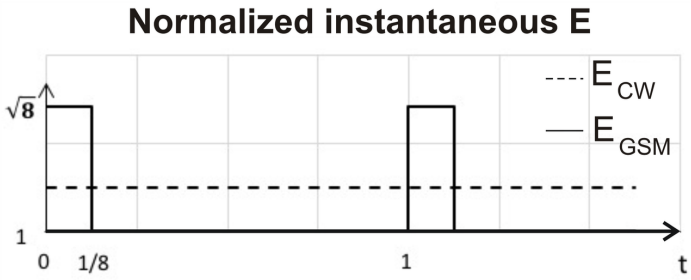
Normalized instantaneous E
√8
1
E CW
E GSM
0
1/8
1
t

C

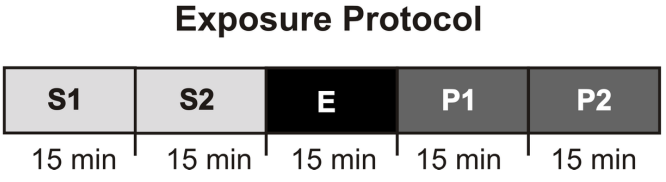
Exposure Protocol
S1
S2
E
P1
P2
15 min
15 min
15 min
15 min
15 min

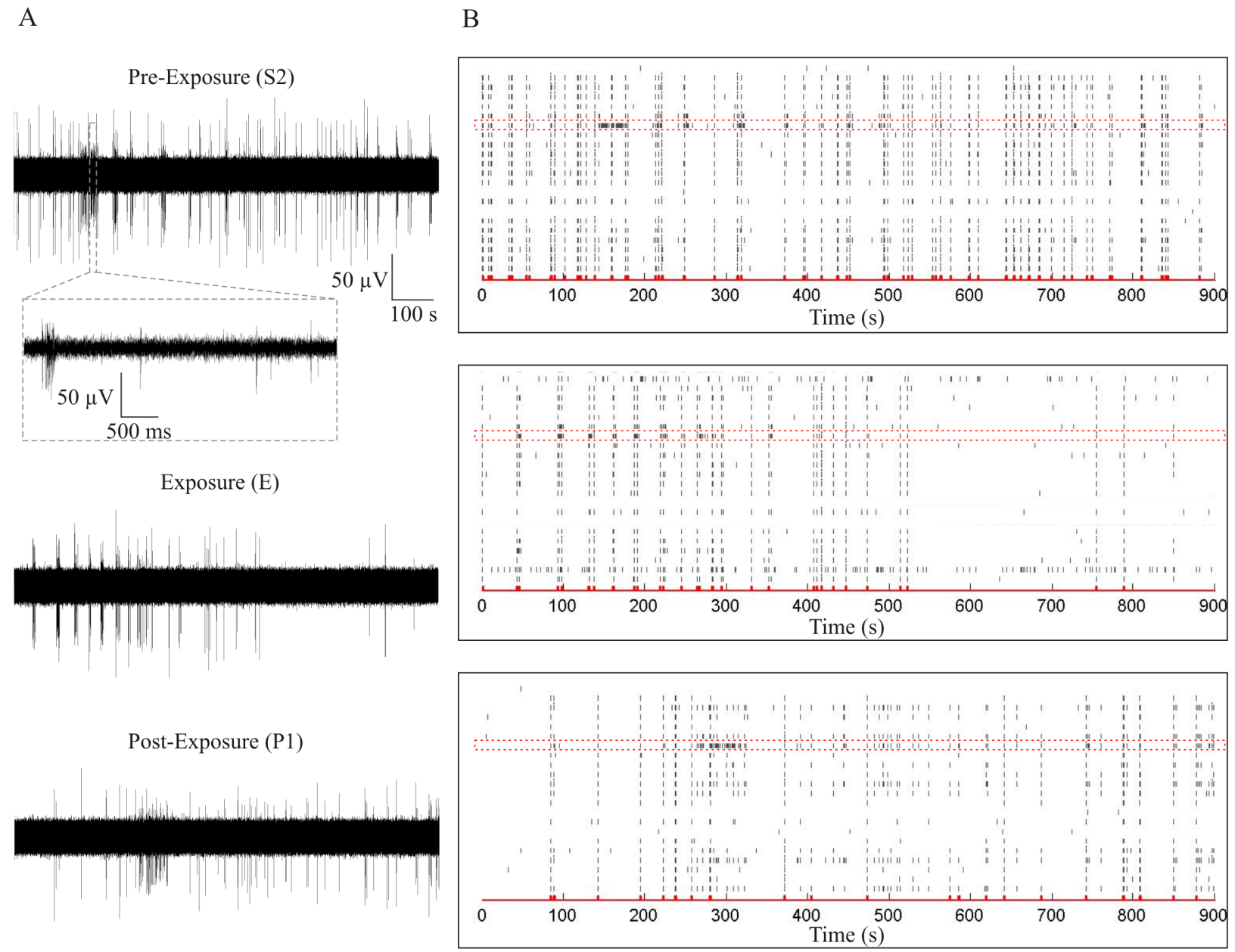
A
B
Pre-Exposure (S2)
50 µV
100 s
50 µV
500 ms
Exposure (E)
Post-Exposure (P1)
0
100
200
300
400
500
600
700
800
900
Time (s)

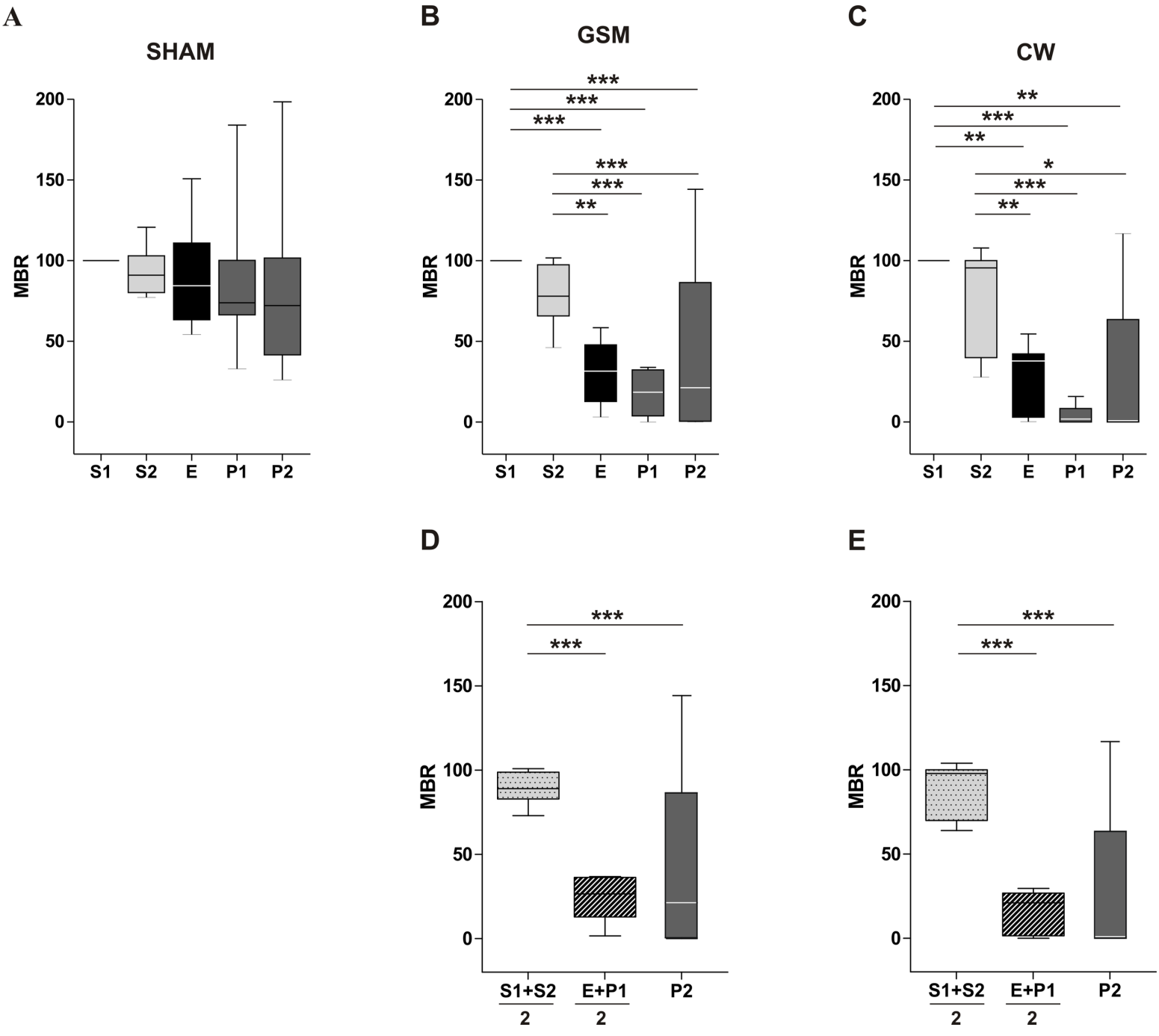
A
SHAM
B
GSM
C
CW
MBR
200
150
100
50
0
S1
S2
E
P1
P2
***
**
*
D
E
S1+S2
2
E+P1
2

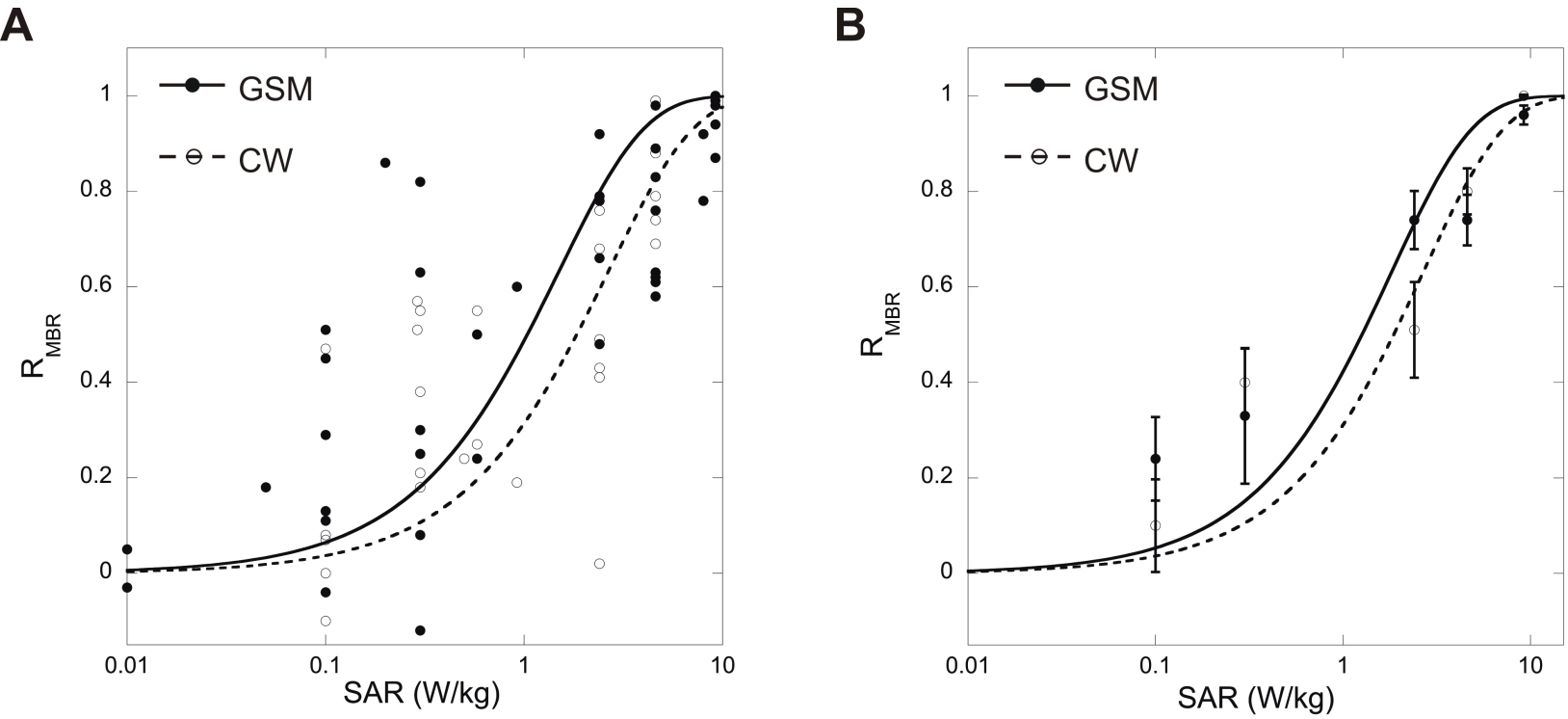
A
B
GSM
CW
R_{MBR}
SAR (W/kg)
0
0.2
0.4
0.6
0.8
1
0.01
0.1
1
10

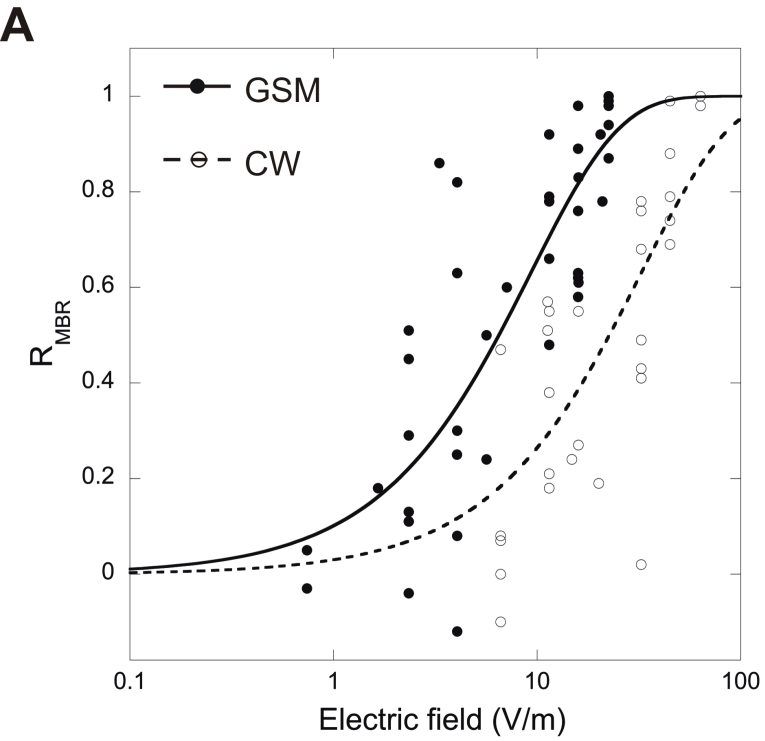
A
GSM
CW
1
0.8
0.6
0.4
0.2
0
R MBR
0.1
1
10
100
Electric field (V/m)

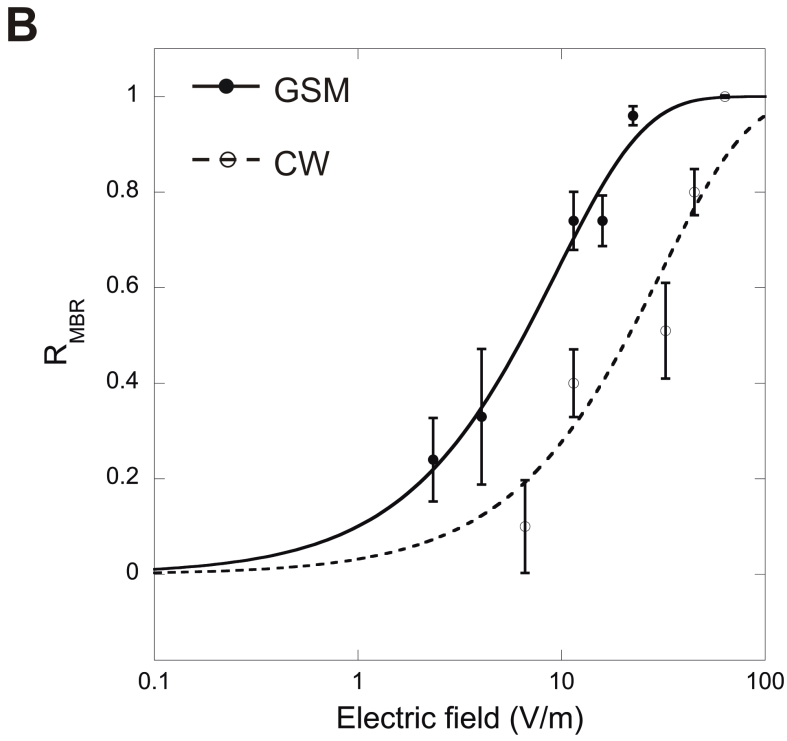
B
GSM
CW
1
0.8
0.6
0.4
0.2
0
R MBR
0.1
1
10
100
Electric field (V/m)

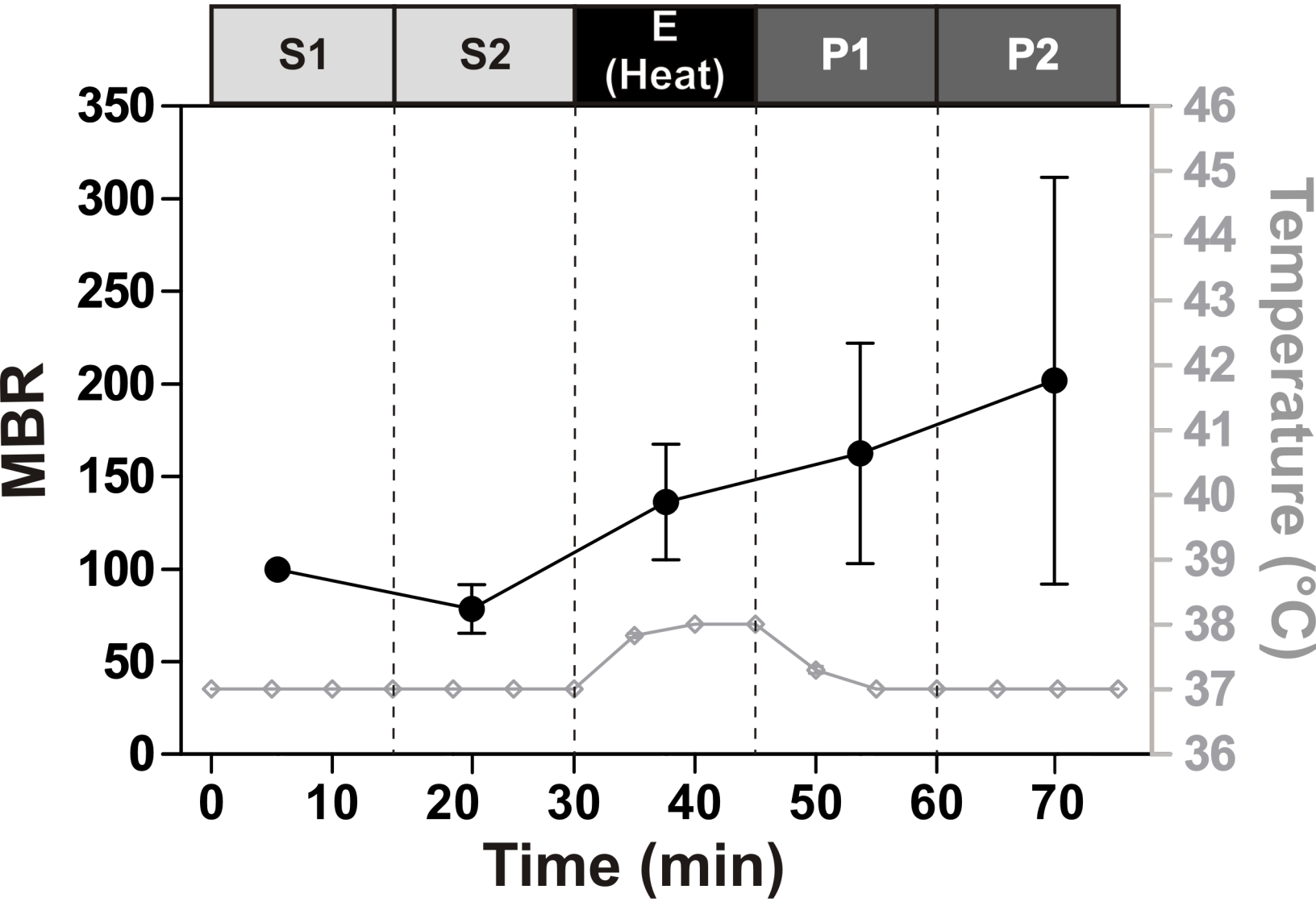
S1
S2
E
(Heat)
P1
P2
MBR
Temperature (°C)
Time (min)
0
50
100
150
200
250
300
350
36
37
38
39
40
41
42
43
44
45
46
0
10
20
30
40
50
60
70